

Recombination dominated Hydrogenic emission from the detached plasmas in W7-AS

N.Ramasubramanian, R.König, U.Wenzel, H.Thomsen, K.McCormick

P.Grigull, Y.Feng, T.Klinger, A.John and the W7-AS Team

Max Planck Institut für Plasmaphysik, EURATOM Association

17491 Greifswald and 85748 Garching, Germany

Introduction

Beyond a certain threshold average density in the **High-Density H-Mode** [1] the island divertor plasma in the stellarator W7-AS undergoes partial detachment. The threshold values, which depend upon the absorbed Neutral Beam Injection heating power are as follows: 2.3 for 0.76 MW, 2.9 for 1.4 MW and 3.5 for 2.5 MW, where the line-averaged density values \bar{n} are in units of $10^{20}m^{-3}$ [2]. The characteristic properties of the HDH mode - flat density profile, edge localized radiation, quasi steady state are still retained even after the detachment except for little changes in the diamagnetic energy and the radiated power. In the detached phase the stored diamagnetic energy is found to be slightly less compared to the same before the transition. The radiated power increases dramatically after the detachment. If the density is ramped up beyond detachment the radiated power increases further following the density until the plasma collapses radiatively thereafter. While the probes, integrated to the target tiles, in the detached locations show a reduction of the ion-saturation current by a factor of about 20 suggesting complete detachment, the plasma is still found to remain attached at some other locations. So in a global sense the stable detachment is said to be partial [2]. But when the island size is small or connection length (L_c) is large the detachment is observed to be complete but very unstable [3]. The neutral pressures monitored by the manometer in the sub-divertor regions display a top/bottom asymmetry with the higher values from the top divertor regions than that of the bottom [4]. The tomographic reconstruction of the radiated power density from the detached pulses show that the radiation profile in the triangular plane is also asymmetric (refer figure 15 in reference [5]). In the detached phase, the spectrometer viewing tangentially to the target tiles in the top divertor region manifests that the impurity radiation layer is close to the X-points. The spectral analysis also demonstrates the presence of a hydrogen radiation zone dominated by recombination emission close to the target tiles. This paper presents the emission from the deeply detached locations including the volume recombination in a stable discharge.

Spectroscopic Diagnostics

The complex nature of the magnetic islands and the island divertor of W7-AS were really challenging for the design of the divertor diagnostics. The interpretation of the data from those regions, particularly the line averaged spectroscopic data are of ambiguous nature. Nevertheless the emission zones of the W7-AS stellarator have been recorded

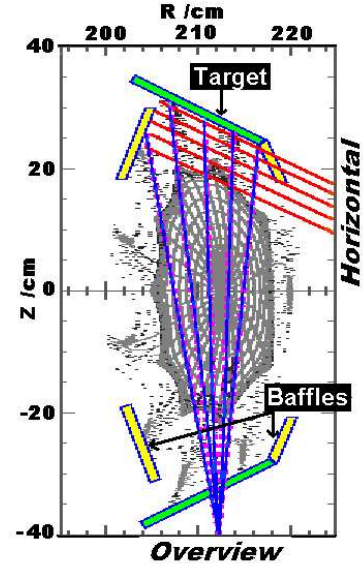


Figure 1: Line of sights for the two spectroscopic systems

with a number of spectroscopy based diagnostic systems. The details can be found in reference [6]. The viewing lines for two systems are shown in figure 1. The first spectrometer, 'Horizontal', views the SOL region tangentially between the target tiles # 8 and # 9 of the top divertor in the Module II. The second one, 'Overview', views across any desired target tile (here it is tile # 5) in the same top divertor module from a bottom port. Both these spectrometers are fitted with two dimensional array detectors which were calibrated for absolute intensities. They were used to monitor the line radiation from impurity ions and hydrogen in the divertor region.

Impurity Radiation Characteristics

In W7-AS carbon is expected to be the main impurity, as the target tiles in the divertor and the baffles are made of carbon. Hence the spectrometers are adjusted to observe the various carbon ionization stages. In the attached HDH mode an intense carbon radiation is identified close to the target tile. During the transition to detachment this radiation front jumps from the location close to the target towards the X-point. Figure 2 shows the transition from the attached to the detached phase in a typical W7-AS discharge as the density (figure 2b) is ramped up. The transition can be readily identified as the moment ($t \sim 0.525s$) at which the stored diamagnetic energy drops to a lower value and the radiated power increases suddenly (figure 2a). The behaviour of the carbon radiation front as recorded by the Horizontal spectrometer

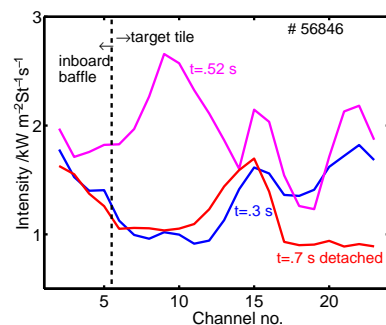


Figure 3: CIII(4647 Å) from the Overview spectrometer across tile # 5 in the top divertor, Module II at three different times - before, at and after the detachment transition

is shown by the intensity of the CIII (4647 Å) line in figure 2c. In the detached phase, the maximum intensity of that line is at $\Delta z \approx 5.5$ cm from the target tile where the X-points are expected from the adjacent islands through the magnetic field calculations. It should be noted that the overall intensity of the CIII radiation after the transition has decreased. The Overview spectrometer viewing the same divertor region from the bottom port though at a different toroidal location (tile # 5) also shows a decrease in the total intensity of the CIII radiation, as shown in figure 3. The CIII emission profile of the detached plasma is fairly flat with slightly more intensity from the channels observing the centre of the target plate and close to the inboard area. The data from the two-dimensional camera equipped with CII filter looking at the bottom divertor from the top port suggests that the radiation from the X-points outside the divertor region actually increases after the detachment [3].

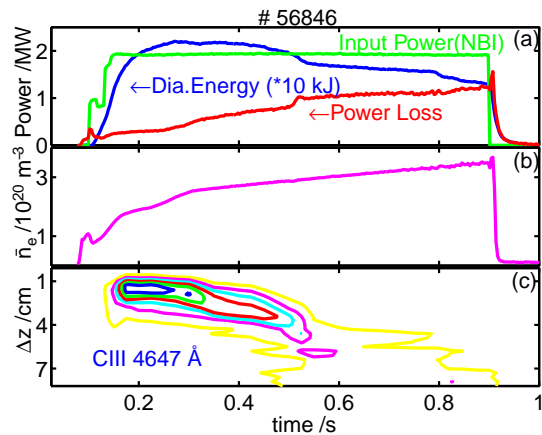


Figure 2: Characteristics during the transition from the attached to the detached phase in a density ramp up discharge (a) Input Power (NBI), Diamagnetic energy, Power loss (from Bolometer), (b) Line averaged density (c) CIII radiation (4647 Å) from Horizontal Spectrometer, Δz is the vertical distance from the target, which is at $\Delta z = 0$.

Balmer Spectra and Volume Recombination

After the detachment, the emission from the region between the target tiles and the impurity radiation layer close to the X-point is found to be consisting mainly of hydrogen. Since the scaling of the population of the different excited levels of hydrogen is different, it is possible to distinguish the contributions from ionizing and recombining plasmas. The ionizing plasma will have heavily populated low- n levels, while the recombination will tend to excite the higher- n levels also to a significant number. The extent of the contributions from recombining or ionizing plasma can be probed by the line ratios of the low- n members as the ratio is very sensitive to recombining and ionizing

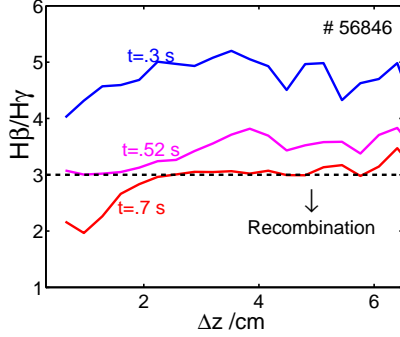


Figure 4: Ratio of H_{β}/H_{γ} ($\leq 3 \Rightarrow$ recombination) from the intensities recorded by Horizontal spectrometer for three different times - before, at and after the detachment transition. Δz , refer figure 2

temperatures. Figure 4 shows the H_{β}/H_{γ} ratio derived from the same pulse at different times. If the ratio is less than 3 (from ADAS, reference [7]) then the emission is dominated by recombination. It can be seen from figure 4 that in the detached phase the plasma in the region $\Delta z \approx 2$ cm, immediately next to the target tile, is dominated by recombination. The increase of the sub-divertor neutral pressure in the top-divertor region also supports the presence of the volume recombination [4]. In W7-AS, the deeply detached discharges could be maintained in quasi-steady state for many energy confinement times. In those discharges the spectrometers were tuned to record the high- n Balmer lines in the wavelength region near the series limit around 3600 Å. Figure 5 shows an example of such a spectrum, which depicts the differences in the spectral characteristics before ($t=0.17$ s) and after detachment ($t=0.37$ s). It can be seen that the spectrum after detachment has detectable line-to-continuum intensities for high- n members ($n \leq 12$). This is indicative of the presence of recombination and low temperature. The individual member lines of the Balmer series are observed to be broadened and the broadening is found to be increasing for higher- n (n -principal quantum number) members. Since the Doppler broadening cannot explain the dependence of full width at half maximum (FWHM) on the principal quantum number and the obtained widths are not expected from the Zeeman effects the broadening is assumed to be due to Stark effects. Thus the n_e values are estimated from the FWHM of the high- n members with the following pre-conditions - the line profiles are distinct with enough line-to-continuum intensities and the FWHM is larger than the instrumental width. Before deducing the density values from the experimental profiles, the instrument contribution has to be deconvolved. The Stark broadened experimental profiles are expected to have Lorentian shapes. Unfortunately

temperatures. Figure 4 shows the H_{β}/H_{γ} ratio derived from the same pulse at different times. If the ratio is less than 3 (from ADAS, reference [7]) then the emission is dominated by recombination. It can be seen from figure 4 that in the detached phase the plasma in the region $\Delta z \approx 2$ cm, immediately next to the target tile, is dominated by recombination. The increase of the sub-divertor neutral pressure in the top-divertor region also supports the presence of the volume recombination [4]. In W7-AS, the deeply detached discharges could be maintained in quasi-steady state for many energy confinement times. In those discharges the spectrometers were tuned to record the high- n Balmer lines in the wavelength region near the series limit around 3600 Å. Figure 5 shows an example of such a spectrum, which depicts the differences in the spectral characteristics before ($t=0.17$ s) and after detachment ($t=0.37$ s). It can be seen that the spectrum after detachment has detectable line-to-continuum intensities for high- n members ($n \leq 12$). This is indicative

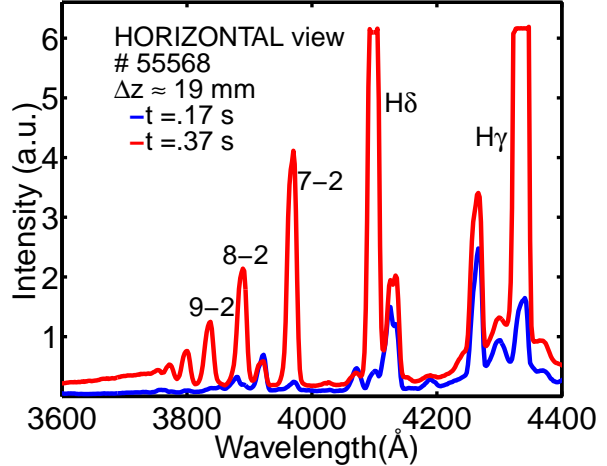


Figure 5: Typical example of the Balmer Spectrum recorded by Horizontal spectrometer from the deeply detached quasi-steady state discharges

the instrument profiles for the both the spectrometers recorded using a discharge lamp in the same wavelength region are found to be asymmetric and the profiles are also found varying for different spatial tracks on the CCD. Since the number of data points are also very small in a given experimental line profile, the deconvolution will be error prone as it involves Fourier transforms. Nevertheless, the asymmetric instrument profiles are approximated by two or three Gaussians which gives the freedom to generate any number of data points. These Gaussian profiles are then convoluted with a Lorentzian profile for a variable n_e value. In this way three (or four) line profiles are fitted simultaneously to the high-n Balmer members with $n=7,8,9$ (and 10). The Stark parameters for these lines are taken from the reference [8]. The intensities (i.e. areas under the individual line profiles) are scaled to a variable temperature assuming Saha-Boltzmann equilibrium. The background continuum is approximated by an arbitrary second order polynomial. The resultant sum of those Balmer member lines and the continuum is fitted to the experimental data by the method of Least Squares by varying n_e and T_e values. A result from such a fit is shown in figure 6. The T_e values for the fitting are found to be in the small range 0.1-0.3 eV, strangely. But the T_e values estimated from the Balmer to Paschen continuum assuming an average density of $1 \times 10^{20} m^{-3}$ are found to be in the range 1.5-3eV. These different values reflect the inhomogeneity of the plasma in the emitting region. The Boltzmann plot is made with only high-n Balmer members and they are originating mainly from the recombining regions. Hence the T_e values from the Boltzmann plot will contain contributions only from the recombining plasma while the continuum ratio will have contributions from all other atomic and molecular processes as well. So the differences in the T_e values from the two different methods are not surprising. The n_e values thus obtained are found to be in the range $3-8 \times 10^{20} m^{-3}$ as shown in figure 7.

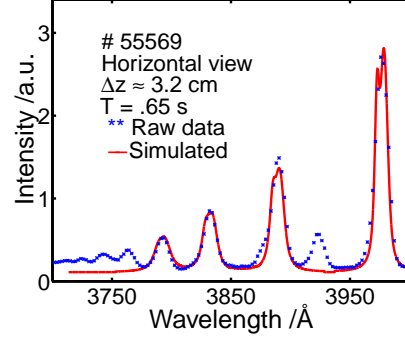


Figure 6: Fitting of a simulated Balmer spectrum, $n_e = 7 \times 10^{20} m^{-3}$ and $T_e = 0.35$ eV.

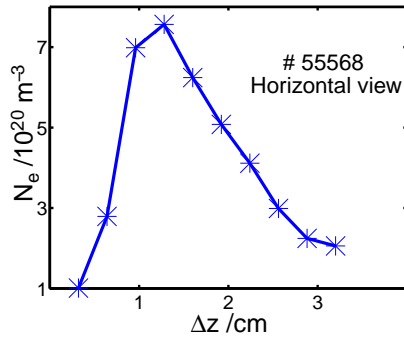


Figure 7: Typical density profile (estimated from Stark broadened high 'n' Balmer members) versus the vertical distance Δz

The density profile shows a peak at a location close to the target tiles and very far away from the impurity radiation region. The conservation of local pressure along the field lines alone cannot explain these very high densities. This density peak is possible only when a source of energy is available locally for ionizing the neutrals. It is not very clear from where it gets energy as the radiation layer close to the X-point would have clipped the energy of the flux crossing it. One can speculate that the locale gets energy from the increased radial transport in the form of "plasma blobs or filaments" ('shoulder' effects in tokamaks [9]) or from the redirection of energy flow around the radiation zone, probably by convective fluxes [10]. Beyond this high density region, there prevail conditions for volume recombination which is evident from the H_β/H_γ ratio close to the target tile as is shown in figure 4. Thus the target receives nearly zero flux

in the detached regions. This volume recombination also thereby increases the neutral pressure locally, which the sub-divertor manometers readily show [4]. With the present understanding, one can conclude that there is no single model with which all these observations can be explained. Hence one needs to think afresh, preferably in three dimensional domains.

Modelling with EMC3-EIRENE Simulation

The improvement towards the realistic reproduction of the experimental results using the EMC3-EIRENE code is still being worked out. The latest being the prediction of the presence of a radiation belt on the inboard side, the details of which can be found in [11]. This result explains the asymmetric power unloading of the target tiles or the partial detachment very well. The experimental results show impurity radiation from all X-points both inboard and outboard. The bolometer data show an asymmetric radiation profile in the triangular plane. The difference in the radiation pattern [12] and the sub-divertor neutral pressure for the normal (-B) and reversed (+B) magnetic field directions (not shown) indicate the influential role of the $E \times B$ drifts. Hence it is expected that after including all the drift effects including the $E \times B$, the simulation might reproduce the observed radiation characteristics and the high density region in front of the target plates. This task is still underway now.

Conclusions

The radiation characteristics of the deeply detached plasmas in the Island divertor of Wendelstein W7-AS Stellarator has been reported here. In the detached phase, the impurity radiation zone is identified to be located near the X-points and hydrogenic emission between the target and the impurity radiation layer. The H_β/H_γ ratio from the SOL region confirms the presence of volume recombination close to the target tiles which plays an important role for complete detachment in the nearby target plates. The analysis of the Balmer spectra obtained suggests that the local physics process are dominating and mandates the importance of three dimensional modelling. While the EMC-EIRENE modelling explains the partial detachment, it does not reproduce the other details like the asymmetric radiation and the high density in front of the target tiles. Further improvements on the code with all drift effects included are expected to explain those details.

References

- [1] McCormick K. *et al* 2002 *Phys. Rev. Lett.* **89**(1) 015001
- [2] Grigull P. *et al* 2003 *J. Nuc. Mater.* **313-316** 1287
- [3] Grigull P. *this workshop* I.Th.4
- [4] McCormick K. *et al* 2002 *Proc. 28th EPS Conf. CFPP (Madera,2001)* **25A** 2105
- [5] Giannone L. *et al* 2003 *Plasma Phys. Controlled Fusion* **45** 1713

- [6] König R. *et al* 2003 *Rev. Sci. Instrum* **74**(3) 2052
- [7] Atomic Data and Analysis Structure *website* - <http://adas.phys.strath.ac.uk/>
- [8] Bengtson R.D. *et al* *Phys. Rev. A* **1**(2) 1970
- [9] Krasheninnikov S.I. 2001 *Phys. Lett. A* **283** 368
- [10] Schneider R. *Private communications*
- [11] Feng Y. *this workshop* I.Fr.3
- [12] Ramasubramanian N. *et al* 2003 *Proc. 28th EPS Conf. CFPP (St.Petersburg,2003)*
P-3.192